Biochimica et Biophysica Acta 940 (1988) 275–287
Elsevier

BBA 74000

Reversible electrical breakdown of lipid bilayers: formation and evolution of pores

Ralf W. Glaser [a,b], Sergei L. Leikin [b], Leonid V. Chernomordik [b], Vasili F. Pastushenko [b] and Artjom I. Sokirko [b]

[a] *Humboldt-University of Berlin, Department of Biology, Berlin (G.D.R.)* and [b] *Frumkijn Institute of Electrochemistry of the Academy of Sciences of the USSR, Moscow (U.S.S.R.)*

(Received 23 November 1987)

Key words: Lipid bilayer; Electrical breakdown; Hydrophobic pore; Hydrophilic pore; Pore formation

The mechanism of reversible electric breakdown of lipid membranes is studied. The following stages of the process of pore development are substantiated. Hydrophobic pores are formed in the lipid bilayer by spontaneous fluctuations. If these water-filled defects extend to a radius of 0.3 to 0.5 nm, a hydrophilic pore is formed by reorientation of the lipid molecules. This process is favoured by a potential difference across the membrane. The conductivity of the pores depends on membrane voltage, and the type of this dependence changes with the radius of the pore. Hydrophilic pores of an effective radius of 0.6 up to more than 1 nm are formed, which account for the membrane conductivity increase observed. The characteristic times of changes in average radius and number of pores during the voltage pulse and after it are investigated.

Introduction

Under the action of high potential differences cell membranes transiently lose their barrier functions (electric breakdown). In the last decade many papers dealt with this phenomenon and its applications in biotechnology and medicine [1,2]. Electric breakdown occurs in the course of electrostimulated fusion and electrotransfection of cells [1,2]. The possible role of this phenomenon, induced by the diffusion potential of the cell membrane, in some pathological process is also discussed [3]. It is generally accepted now that electrical breakdown is based on the formation of pores in the lipid areas of the membrane. However, there is no common view on their structure and on the mechanism of their formation [1–10]. From our point of view in this situation the study of electroporation mechanism and phenomenology by means of simple model systems based on planar lipid bilayers is especially important.

In this paper the results of theoretical and experimental studies of reversible electric breakdown of lipid bilayers are presented. The formation of short-living small hydrophobic pores is shown to be a first stage of electroporation. Then inversion of the pore edge occurs. As a result hydrophilic pores, determining the membrane conductivity are formed. The evolution of these pores is investigated. The dependence of the rate of hydrophilic pore creation on the voltage applied is quantitatively described. The time course of the changes in number and average size of hydrophilic pores during and after voltage pulses is studied by means of quantitative analysis of the membrane current-voltage characteristics.

Correspondence: R.W. Glaser, Humboldt-Universität zu Berlin, Institut für Medizinische Immunologie, Schumannstrasse 20/21, Berlin, 1040 G.D.R.

Theory

Energy of a hydrophobic pore

We assume that the mechanism of electroporation is the following: Owing to thermal motion of lipid molecules hydrophobic pores are spontaneously formed in the lipid matrix (Fig. 1a). The probability of the existence of a hydrophobic pore is determined by the dependence of pore energy on pore radius. When these pores exceed the critical size, a reorientation of the lipids converts the pores into hydrophilic ones with the head groups forming the pore walls (Fig. 1b).

Let us determine the change of free energy resulting from the formation of a cylindrical hydrophobic pore of the radius R in a lipid bilayer. This free energy E_o is termed the energy of the pore. The pore is filled with water.

Earlier papers used to calculate E_o from [4]

$$E_o = 2\pi R h \sigma_o(\infty) \tag{1}$$

where h is the thickness of the membrane and $\sigma_o(\infty)$ is the interface tension between hydrophobic lipid tails and water. From Eqn. 1 the energy of a hydrophobic pore of 0.5 nm radius was calculated in the order of 200 kT (with $h = 5$ nm and $\sigma_o(\infty) = 0.05$ N/m). It was concluded that the spontaneous formation of hydrophobic pores as a stage of hydrophilic pores arising was highly unprobable [4].

In Eqn. 1, however, the interaction between the walls of the pore has not been regarded. Recently, Israelachvili and Pashley [11] showed experimentally that the interaction of two hydrophobic surfaces separated by a thin layer of water significantly reduces the interface tension σ_o. The reduction of σ_o was attributed to changes in water structure near the interface with hydrophobic substances as follows. From the interface to the bulk phase the properties of water undergo a gradual

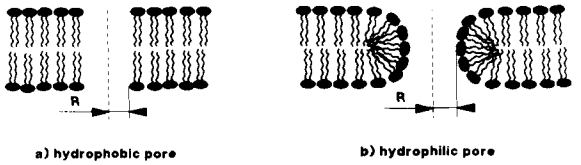

Fig. 1. Types of pore in lipid membranes.

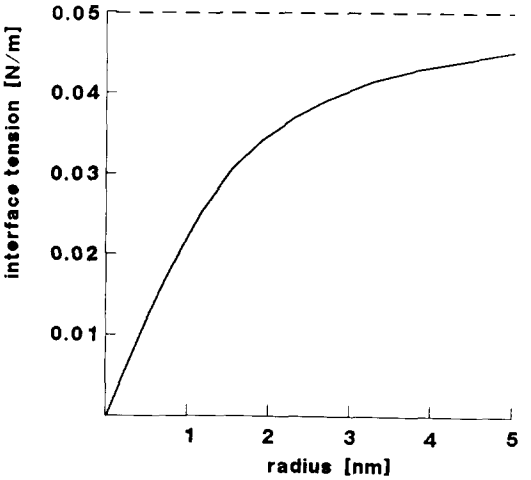

Fig. 2. Effective interface tension between hydrophobic pore wall and water as a function of pore radius. The data are calculated from Eqn. 2 with $\sigma_0(\infty) = 5 \cdot 10^{-2}$ N/m and $\rho = 1$ nm. The dashed line shows the interface tension $\sigma_0(\infty)$ without hydrophobic interaction.

transition with a characteristic length ρ of 1 nm [11]. The high interface tension originates from the excess energy of this thin layer with disturbed water structure. When two hydrophobic surfaces come to a distance of a few nanometers the overlapping of these layers reduces the effective surface tension σ_o and causes hydrophobic attraction between the surfaces [11,12].

Based on the theoretical model that was suggested by Marcelja [12] we calculated the effective value of $\sigma_o(R)$ and the pore energy $E_o(R)$ (see Appendix),

$$\sigma_o(R) = \sigma_o(\infty) I_1(R/\rho)/I_0(R/\rho) \tag{2}$$

$$E_o(R) = 2\pi h R \sigma_o(R) \tag{3}$$

where $I_n(x)$ are modified Bessel functions of n-th order. σ_o as a function of R is shown in Fig. 2. At $R \gg \rho$ is $\sigma_o(R) \approx \rho_o(\infty)$, while at $R \ll \rho$ is $\sigma_o(R) \approx R\sigma_o(\infty)/2\rho$ with $\sigma_o(R = 0) = 0$.

In Fig. 3 the pore energy E_o is shown as a function of R according to Eqn. 1 and Eqn. 3. It is obvious that the interaction of the pore walls significantly reduces the energy of the hydrophobic pores. For example, at $R = 0.5$ nm the energy is reduced to one fifth.

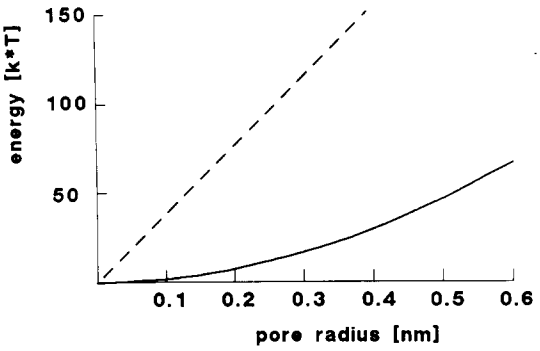

Fig. 3. Energy of hydrophobic pores as a function of pore radius. — — —, without consideration of hydrophobic interaction between pore walls; ———, under consideration of hydrophobic interaction according to Eqn. 3.

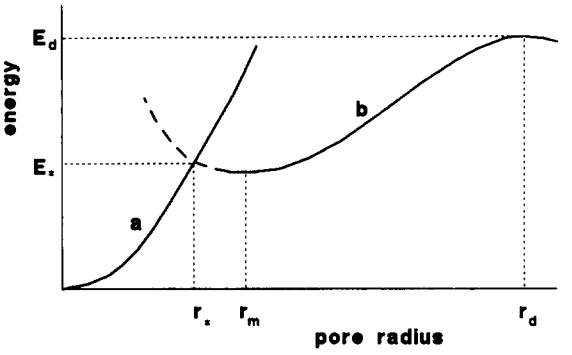

Fig. 4. Comparison of the energy of hydrophobic and hydrophilic pores at different pore radii. (a) hydrophobic pores; (b) hydrophilic pores. A hydrophobic pore of zero radius is identical with the undisturbed state of the membrane – the energy is zero. Hydrophilic pores of small radius have high energies. At a radius r_* the energies of hydrophobic and hydrophilic pores are equal; this energy E_* is the minimal energy that has to be overcome to form a hydrophilic pore. The radius r_m, where hydrophilic pores have minimal energy, may be larger than r_*; under these conditions hydrophilic pores can exist in a metastable state. If the radius of the pore becomes larger than r_d the pore will grow indefinitely and destroy the membrane.

Energy of a hydrophilic pore

The energy of a hydrophilic pore is generally calculated from [13,14]

$$E_i = 2\pi\gamma R - \pi\sigma_b R^2 \tag{4}$$

where γ is the edge energy of the pore walls and σ_b is the effective mechanical tension of the membrane. R is understood as the radius of the narrowest part of the channel in the membrane (Fig. 1b).

However, for pores with small radius ($R \ll h$) Eqn. 4 with constant γ is inapplicable [4,5,15,16]. The packing of lipids along the wallside of a narrow pore leads to substantial deformation of the molecular order. The contribution of this deformation to pore energy steeply rises when R approaches the size of the lipid heads [4,16]. In addition, strong hydration interaction [17] causes repulsive forces between the hydrophilic compounds of the pore wall. Both effects lead to an increase of E_i at small radius. Since the precise dependence of E_i on small radii is unknown, we can only give the qualitative description. The dependence is assumed to have the form shown in Fig. 4 [4]. The local minimum of E_i is expected around $R_m \approx 1$ nm.

Hydrophilic pore formation

The comparison of $E_o(R)$ and $E_i(R)$ shows that the formation of hydrophobic pores in the bilayer is energetically more favourable if the radius is very small (Fig. 4). These hydrophobic pores are formed spontaneously by lateral thermal fluctuations of the lipid molecules. But when their radius exceeds a critical value R_*, at which $E_o(R_*)$ equals $E_i(R_*)$, a reorientation of the lipids becomes energetically favourable. This reorientation, resulting in the formation of a hydrophilic pore, will be called the inversion of the pore. The life time of the hydrophobic pores is in the order of the lipid fluctuations; they are only intermediate stages in the formation of hydrophilic pores.

Accumulation of hydrophilic pores in the membrane due to an electric field is considered to be the reason for reversible electric breakdown [9]. Assuming additional energy of intermediate steps of the inversion to be negligible we find the energy barrier which has to be overcome for hydrophilic pore formation,

$$\Delta W_p(U = 0) = E_o(R_*) \tag{5}$$

The rate K_p, at which metastable pores are spontaneously formed, is calculated according to Ref. 13,

$$K_p = \frac{\nu S}{a_o} \exp\left(-\frac{\Delta W_p}{kT}\right) \tag{6}$$

where S is the area of the membrane, a_o the area per lipid molecule, and ν the frequency of lateral fluctuations of the lipid molecules, since the rate at which the pore can open is mainly determined by lipid fluctuations.

Equations 5 and 6 are valid as well when the voltage across the membrane differs from zero. The dependence of cylindrical hydrophobic pore energy on membrane voltage can be expressed in the form [5,14],

$$E_o(U, R) - E_o(0, R) = -\frac{\pi R^2(\varepsilon_w - \varepsilon_m)\varepsilon_0 U^2}{2h} \quad (7)$$

where ε_w is the relative permittivity of water inside the pore, ε_m the relative permittivity of the membrane and ε_0 the dielectric constant of the vacuum.

From Eqns. 4–7 we get

$$\ln K_p(U) = \ln\left(\frac{\nu S}{a_o}\right) - \frac{\Delta W_p(U=0)}{kT} + \frac{\pi R_*^2(\varepsilon_w - \varepsilon_m)\varepsilon_0 U^2}{2hkT} \quad (8)$$

If we assume, according to Ref. 14, that the dependence of $E_i(R)$ on U is also described by Eqn. 7, we obtain that R_* is constant and independent of U. However, for real noncylindrical hydrophilic pores we should expect that the dependence $E_i(U)$ slightly differs from Eqn. (7). Nevertheless, the steep decrease in $E_i(R)$ for $R > R_*$ (Fig. 4) allows us to neglect the influence of U on R_* caused by this difference. The fact that R_* is independent of U allows us the experimental verification of Eqn. 8 and the theory developed.

Let us briefly discuss the ways of further evolution of hydrophilic pores in planar lipid bilayer membranes. When $U = 0$, it follows from Eqn. 4 that the pore growth is hindered by an energy barrier (Fig. 4) [13,14]. The height ΔW_d and the coordinate R_d of the barrier top can be estimated as $\Delta W_d = \pi\gamma^2/\sigma_b$ and $R_d = \gamma/\sigma_b$. An electric field reduces the barrier. To estimate $W_d(U)$ and $R_d(U)$ Eqn. 7 is usually applied to $E_i(R)$ [14]. Taking for $R > R_m$ $\gamma \approx 10^{-11}$ N [18,19]; $\varepsilon_w \approx 80$; and $h \approx 5$ nm, we find that for high voltages ($U \approx 0.5$–1 V) the energy barrier for pore growth disappears. This, in principle, means that hydrophilic pores should grow infinitely and that the breakdown should be irreversible. So the question arises why some planar lipid bilayer membranes of special composition demonstrate the reversible breakdown at high voltages. One reason of such behaviour can be very high viscosity of this membranes preventing fast growth of the pore [20].

The other reason can be crucial as well. The situation changes drastically for membranes with $\sigma_b \ll \gamma/h$. Eqn. 7 is valid only for narrow pores ($R \ll h$), and can not be applied, even qualitatively, for $R > h$. Consequently, Eqn. 7 can not be applied in the region of $R \approx \gamma/\sigma_b$, where the energy barrier for pore growth is situated according to the equation. It has been shown that in this case the energy barrier can remain high enough to prevent the irreversible rupture of the membrane even at high voltages [21]. It is natural to suggest that this is the case where reversible breakdown is observed.

Pore conductivity

The dynamics of pore development are of substantial interest for understanding the mechanism of reversible electric breakdown.

Information on pore size can be drawn from the dependence of membrane conductivity on membrane voltage [22]. The character of this dependence is determined by the pore size. While the conductivity of small pores rapidly grows when the voltage rises, large pores are nearly ohmic. Thus it appears to be possible to estimate the number and the size of the pores from conductivity measurements at different voltages (Fig. 6). These calculations are based on the model proposed in Ref. 22, which is presented below.

We assume that the conductivity of the membrane is produced by pores of identical size and shape. Such an 'average' pore is shown in Fig. 5. The external radius of the channel entrance is R_o. The inner radius R, i.e. the radius of the pore is small in comparison with the membrane thickness h. The conductivity of the pore G can be calculated as the conductivity of a cylindrical channel of the radius R_o that represents an energetic barrier for ions. The shape of this barrier is determined by the real structure of the pore walls (Fig. 5). The maximum height of the barrier is produced by the interaction of an ion with the surrounding membrane material at the narrowest part of the pore.

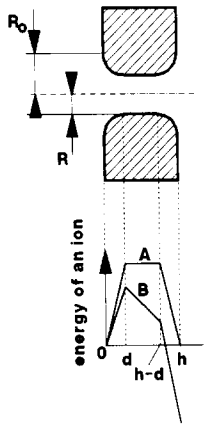

Fig. 5. Simplified energy profile of a hydrophilic pore: energy of an ion crossing the membrane as a function of its position along the axis of the hydrophilic pore. Inside the pore the energy of the ion is increased due to the interaction of the ionic charge with the low permittivity areas of the membrane. The energy profile can be approximated by a trapezium (A), this enables the calculation of pore conductivity by Eqn. 10. If a voltage is applied to the membrane, the energy barrier for ions will decrease (B).

According to Ref. 22 the conductivity of the membrane in the solution of an 1 : 1 electrolyte is calculated from

$$G = \pi R_o^2 \mathscr{K} N \frac{\exp(\beta U) - 1}{U \int_0^h \exp\left[\beta U \frac{h-x}{h} + w(x)\right] dx} \tag{9}$$

where U is the potential difference across the membrane, N the number of pores, $\mathscr{K}$ the specific conductivity of the bulk solution, $\beta = e/kT$ and $w(x) = W(x)/kT$, where e is the electron charge and $W(x)$ the energy of an ion inside the pore in dependence on the distance from one surface of the membrane. We assume that the shape of the energy barrier is a trapezium [22] (Fig. 5). For $\beta U \gg 1$ ($U \gg 25$ mV) we get

$$\ln G = \ln \frac{\pi R_o^2 \mathscr{K} N}{h} - \ln\left[\left(1 + \frac{n\beta U}{w_0 - n\beta U}\right) \exp(w_0 - n\beta U) - \frac{n\beta U}{w_0 - n\beta U}\right] \tag{10}$$

where $n = d/h$ is the relative size of the entrance region of the pore (Fig. 5) and w_0 the energy of an ion in the center of the pore in units of kT. Eqn. 10 is in accordance with the experimentally observed dependence of ln G on U [22].

According to Eqn. 10 the membrane conductivity depends on the three parameters $\pi R_o^2 \mathscr{K} N/h$, n, and w_0. As long as the radius of the pores is small in comparison with the membrane thickness ($R \ll h$), one can assume that $R_o \approx h/2$ is independent of R (Fig. 5). Changes in the first parameter $\pi R_o^2 \mathscr{K} N/h$, therefore, are mainly due to a change in the number of pores in the membrane. These changes only cause a vertical shift of the ln G-curve without affecting the shape of this curve. The second parameter – the relative entrance length n – affects the shape of the ln $G(U)$ curve. Particularly, n determines the slope of ln $G(U)$ at small voltages. For $n\beta U \ll w_0$ and $w_0 \gg kT$ Equation (10) provides

$$\ln G = \ln \frac{\pi R_o^2 \mathscr{K} N}{h} - 0.43 w_0 + 0.43 n \beta U \tag{11}$$

When we suppose that $R \ll h$, the relative entrance length n is basically defined by the shape of the pore wall (Fig. 5) and is nearly independent of the radius. Consequently, n can be assumed as a constant at membranes of the same type.

Thus the maximum energy of an ion in the pore w_0 is the only parameter influencing the course of ln $G(U)$ for a given membrane. On the other hand w_0 is immediately connected with the radius of the narrowest part of the pore R. When the radius of the pore is decreased, the energy of an ion inside the pore increases because of the interaction with the surrounding membrane of low dielectric constant [23]. For example, for infinitely long cylindrical pores with $\varepsilon_m = 2$ and $\varepsilon_w = 80$, R can be approximated by

$$R = 5nm/w_0 \tag{12}$$

as it has been shown by Parsegian [23].

Consequently, it is possible to obtain information about the dynamics of pore size and pore number from w_0 and N which are provided by fitting Eqn. 10 to the measured dependence of membrane conductivity on voltage.

Materials and Methods

Membranes

Membranes were formed from 10 mg asolectin (Sigma) per ml decane in the usual way on the orifice of a two-compartment teflon chamber filled with 100 mM KCl. The temperature was 30 °C. After the membrane had grown black, uranyl ions were added in small portions of $UO_2(CH_3COO)_2$ solution to both compartments up to a final concentration of 10^{-3} M. Experiments were carried out 15 to 30 h after the preparation of the membrane.

The current flowing through the membrane was measured during voltage pulses consisting of two or more rectangular parts. Details of the device have been described by Chernomordik et al. [20]. Pulses were given in intervals of at least 2 minutes.

Rate of pore creation

We determined the dependence of the rate of formation of metastable hydrophilic pores K_p on the voltage U_t of the test pulse.

The membrane was exposed to pulses composed of three rectangular parts (Fig. 6). The first part and the third part were measuring pulses of equal voltage U_m, which was not changed during a set of experiments. The second part was the test pulse with variable voltage U_t and length Δt. The difference of current $\Delta I = I_2(U_m) - I_1(U_m)$ immediately after and before the test pulse was analysed under the measuring voltage U_m (see Results). The value of I_2 was obtained by extrapolation of the current $I(t)$ of the third part to the end of the test pulse.

Determination of pore size and number

The membrane was exposed to pulses composed of a test pulse and a measuring part. The conductivity of the membrane that was induced by the test pulse was determined as a function of the measuring voltage. Therefore, series of experiments were performed in which immediately after an identical test pulse a short measuring pulse of variable voltage was given (Fig. 7). The conductivity was extrapolated to the beginning of the measuring pulse to remove capacitive currents and conductivity changes during the measuring pulse.

Such series of experiments were carried out with test pulses of different length and voltage. In addition, experiments were performed in which the measuring pulses were given at various intervals after the test pulse. In all cases the conductivity during the test pulses was controlled to exclude changes in the electric properties of the membrane that might arise from extensive pulsation.

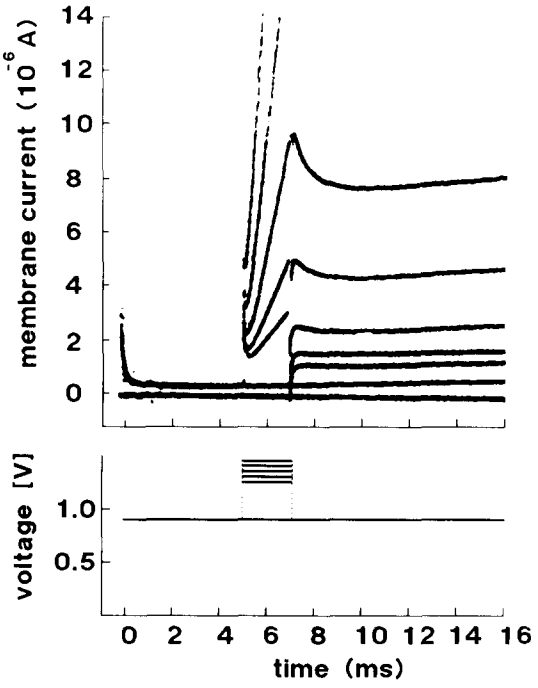

Fig. 6. Experimental determination of the rate of pore creation: oscillogram of membrane current and voltage pulse applied to the membrane. The current tracks of six pulses and a zero line are shown in one oscillogram. Each pulse consists of three parts: (1) 5 ms of $U_m = 900$ mV, (2) 2 ms of variable voltage ($U_t = 900$–1450 mV) and (3) 9 ms of $U_m = 900$ mV. While the traces of the first parts fall together the different voltages of the second parts causes different current traces of the third parts. At 7–9 ms the current is influenced by changes in pore size, therefore the linear part is extrapolated to 7 ms. The difference between this extrapolation and the current of the first part at 5 ms provides the increase of membrane current ΔI resulting from pore creation by the second part of the pulse.

From the relation between membrane conductivity and voltage the energy w_0 and the number of pores N were derived. These parameters were fitted in a way that Eqn. 10 satisfied the measured data with least-square deviations in $\ln G$. The other parameters were set $h = 5$ nm, $R_o = h/2$, and $\mathscr{K} = 1.3$ S/m.

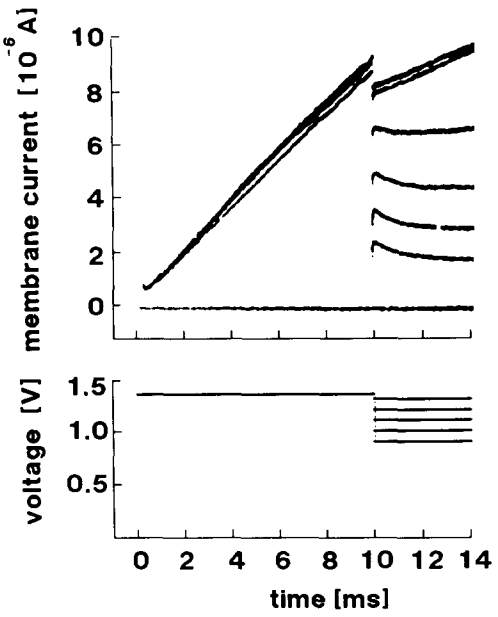

Fig. 7. Measurement of the voltage dependence of pore conductivity for the determination of pore size: oscillogram of membrane current and voltage pulses applied to the membrane. Pulses consist of a 10 ms part of constant voltage (1350 mV) to put the membrane to the desired state for investigation and of a 4 ms part of variable voltage (900–1300 mV) to investigate the current-voltage characteristic of the membrane in this state. In these experiments only the first 0.2 ms of the second part (capacitive currents) are neglected by extrapolation. The first pulse (1350/1300 mV) is repeated after the experiment to estimate the extent of membrane damage due to the pulses.

The relative entrance length n was supposed to be constant. The best correspondence between experimental and theoretical data was achieved with $n = 0.15$.

Lysophosphatidylcholine treatment

Uranylized membranes were made as described above. After 15 to 20 h, under continuous stirring, lysophosphatidylcholine from egg yolk (Serva) was added to both sides of the membrane up to a final concentration of 5 μg/ml. The current flowing through the membrane, which was the response to identical rectangular voltage pulses, was studied after different time intervals and compared with the response before lysophosphatidylcholine was added.

Lysophosphatidylcholine was used in a solution of 2 mg per ml ethanol. Addition of an adequate amount of ethanol without lysophosphatidylcholine did not have any effect on membrane properties.

Results and Discussion

Characterisation of the energy barrier for hydrophilic pore formation

We found the dependence of $\ln(\Delta I/\Delta t)$ on U_t^2 by the application of pulses of a voltage U_t from 0.65 to 1.9 V (Fig. 8).

In the range between 0.65 and 1.5 V the current through the membrane increased linearily during the test pulse. Thus the rate of pore death was low in comparison with the rate of pore formation and could be neglected. We assumed that $\Delta I(U_t) =$

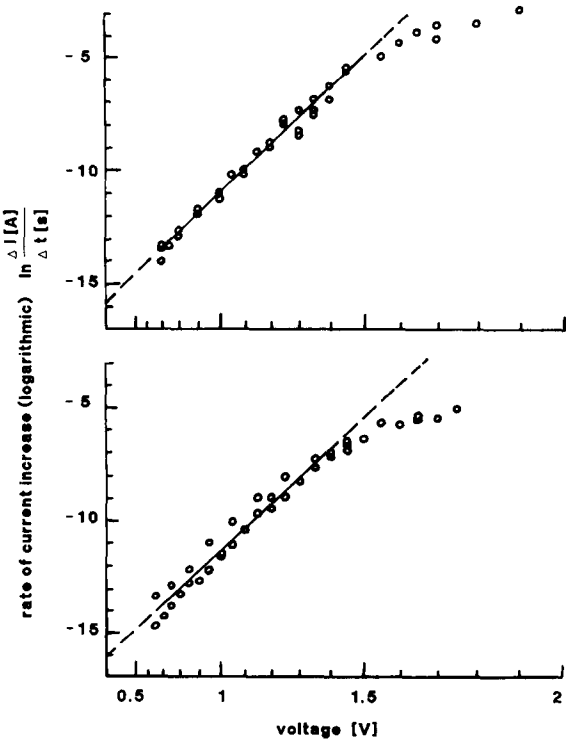

Fig. 8. Dependence between the logarithm of the rate of current increase $\Delta I/\Delta t$ and the square of the voltage U_t of the test pulse. The current was measured in two individual membranes at a constant voltage of $U_m = 900$ mV and 800 mV, respectively. Increasing the voltage U_t from 0.65 to 1.9 V the length Δt of the test pulse was decreased from 100 ms to 0.1 ms. Linear regression of the data at $U_t \leqslant 1.45$ V provided for $\ln(\Delta I/\Delta t) = A + B \cdot U_t^2$ $A = -15.9$, $B = 4.8$ V^{-2} and $A = -16$, $B = 4.7$ V^{-2}, respectively.

$\Delta N(U_t) \cdot U_m g(U_m)$, where $\Delta N(U_t)$ is the number of hydrophilic pores that were formed in the bilayer by the test pulse and $g(U_m)$ is the average conductivity of the pores at $U = U_m$. Accordingly, the rate of pore formation is

$$K_p(U_t) = \frac{\Delta I(U_t)}{U_m g(U_m) \Delta t} \tag{13}$$

where Δt is the length of the test pulse. From Eqn. 13 we find that for comparison with the experimental data the theoretical Eqn. 8 can be presented as

$$\ln \frac{\Delta I}{\Delta t} = A + B U_t^2 \tag{14}$$

where

$$A = \ln \frac{U_m g(U_m) \nu S}{a_0} - \frac{\Delta W_p(U=0)}{kT} \tag{15}$$

and

$$B = \frac{\pi R_*^2 (\varepsilon_w - \varepsilon_m) \varepsilon_0}{2hkT} \tag{16}$$

Here we assume the pore conductivity $g(U_m)$ to be independent of the amplitude U_t and duration Δt of the test pulse. The value of $g(U_m)$ is determined by the average pore size, which depends on U_t and on Δt. (Δt was varied from 100 ms at $U_t = 0.65$–0.7 V to 0.1 ms at $U_t = 1.7$–1.9 V). However, the dependence of $\ln(\Delta I/\Delta t)$ on $g(U_m)$ is very weak in comparison with the dependence on U_t^2. For example, changes in $g(U_m)$ by a factor of 3–5 lead to changes in $\ln(\Delta I/\Delta t)$ which are within the experimental accuracy (Fig. 8). Besides, to determine ΔI the current $I(t)$ of the second measuring pulse was extrapolated to the end of the test pulse (Fig. 6). Thus, $g(U_m)$ corresponds to the pore size after about 10 ms relaxation under standard measuring conditions ($U = U_m$). This relaxation significantly reduces the influence of U_t and Δt on $g(U_m)$.

Fig. 8 shows that in the range $0.65\ \text{V} < U_t < 1.5$ V the dependence of $\ln(\Delta I/\Delta t)$ on U_t^2 is linear as predicted theoretically.

By linear regression of $\ln(\Delta I/\Delta t)$ against U_t^2 the parameters A and B were calculated: $A = -15.9$, $B = 4.8\ \text{V}^{-2}$ at $U_m = 900$ mV (membrane I) and $A = -16.0$, $B = 4.7\ \text{V}^{-2}$ at $U_m = 800$ mV (membrane II).

From parameter B the critical radius R_* can be determined, at which the energy barrier for the formation of hydrophilic pores is situated. With $T = 300$ K, $h = 5$ nm and $\varepsilon_w - \varepsilon_m = 80$, Eqn. 16 provided $R_* \approx 0.3$ nm. We are aware, however, that this is a rough determination. The uncertainty arises from the simplification of the model: the continuous description is applied to the discrete molecular structure. In addition, the dielectric properties of the water inside the pore differ form the bulk phase, and ε_w is probably below 80.

From parameter A the energy of the barrier for the formation of hydrophilic pores was calculated. Assuming that $g(U_m) \approx 10^{-11}$ S (see below), $\nu \approx 10^{11}\ \text{s}^{-1}$, $S = 1\ \text{mm}^2$, and $a_0 = 0.6\ \text{nm}^2$, Eqn. 15 provided $\Delta W_p(U=0) \approx 45\ kT$. Although g and ν are only known by the order of magnitude, the error of ΔW_p can hardly exceed 10 kT, because ΔW is proportional to the logarithm of these parameters.

Since $\Delta W_p(U=0) = E_o(U, R_*)$, Eqn. 3 could be employed for an independent determination of the critical radius with $R_* \approx 0.5$ nm (Fig. 3). Considering the limited accuracy mentioned above this result is in accordance with the value calculated from parameter B. It should be noted that the parameters A and B refer to quite different aspects of the pore formation process. The two determinations of R_* are independent and thus their correspondence supports the proposed model of pore formation.

At test pulses above 1.5 V $\ln(\Delta I/\Delta t)$ more and more deviated from the linear dependence (Fig. 8). Simultaneously the current increase during the test pulse became non-linear. These divergences result from voltage drop in the bathing solutions produced by the high membrane currents. When the current flowing through the membrane exceeded 10^{-4} A the membrane voltage was reduced by more than 100 mV because the resistance of the bathing solutions was 1.5 kΩ. The divergences do not reflect any changes in the pore formation properties of the membrane.

An additional information can be obtained from the experiments described. From Fig. 6 one can draw that the membrane has a substantial back-

ground conductivity (about $3 \cdot 10^{-7}$ S). We obtain this value by extrapolation of $I(t)$ to the beginning of the first measuring pulse with $U = U_m$ (Fig. 6).

The high background conductivity of the membrane can not arise from hydrophobic pores because of their short life time. The probability that the membrane has a 0.5 nm hydrophobic pore is very small (about 10^{-6} in an area of 1 mm^2). Let us assume that the high background conductivity of the membrane is due to an equilibrium population of hydrophilic pores existing in the membrane [16]. The mean number of such pores at $U = 0$ is equal to $N_e = \tau_r K_p(U = 0)$, where τ_r is the mean time of pore resealing. This relation can be used to estimate the value of τ_r. N_e is given by $N_e \approx I_b/(U_m g(U_m))$, where $g(U_m)$ is the mean pore conductivity at $U = U_m$. From Eqns. 13–16 we find that $K_p(U = 0) = \exp(A)/(U_m \cdot g(U_m))$. Therefore τ_r can be expressed as

$$\tau_r = I_b \exp(-A) \tag{17}$$

Substituting $I_b \approx 3 \cdot 10^{-7}$ A and $A = -16$ we get $\tau_r \approx 3$ s.

Note that to obtain Eqn. 17 only two model assumptions have been used: (i) that the background conductivity is determined by pores; and (ii) that the conductivity of background pores and pores created by the test pulse are nearly equal at $U = U_m$.

Further evolution of the pores

By special experiments Chernomordik et al. [22] have shown that the dependence of conductivity on voltage, obtained by the method described, is based on nonohmic behaviour of hydrophilic pores rather than on changes of their mean size or number.

Fig. 9 shows the dependence of $\ln G$ on U measured after pulses of various length. Obviously, Eqn. 10 is able to describe these experimental data quite exactly. The parameters w_0 and N, which are determined from the fits, give us an understanding of the evolution of the population of pores in the membrane during and after the pulse. In the following the dependence of w_0 and N on length and voltage of the pulse will be discussed in detail.

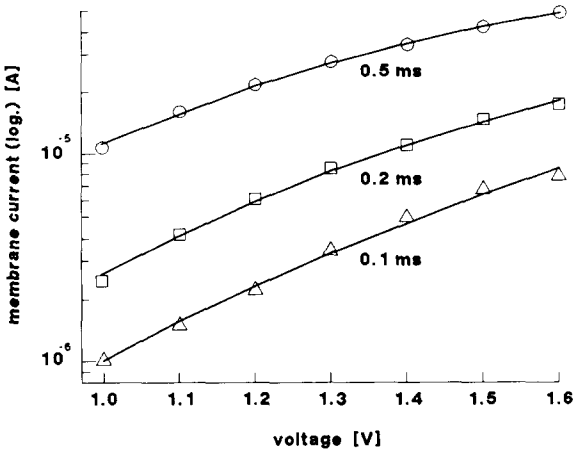

Fig. 9. Relationship between membrane current and voltage immediately after pulses of 1.6 V and a duration of 0.1 ms (△), 0.2 ms (□), and 0.5 ms (○) (experimental data). The experiment was performed as demonstrated in Fig. 7. ———, fitted according to Eqn. 10. Parameters drawn from the fit see right column of Table I.

An increase of the pulse length Δt leads to a proportional increase of the number N of pores in the membrane (Table I). This is in good agreement with the results obtained above. Simultaneously, the energy of an ion in the pore w_0 is decreased (Table I), i.e., the radius of the pore increases during the pulse. Rough estimation by

TABLE I

DEPENDENCE OF PORE SIZE AND NUMBER ON THE PARAMETERS OF THE PULSE

The energy barrier w_0 for univalent ions crossing the membrane and the number of pores N are compiled in dependence on the pulse length. The current-voltage characteristic of an uranylized membrane was measured as described in Fig. 7 and both parameters were calculated by a nonlinear regression program based on Eqn. 10. The data after 1.45 V and 1.6 V pulses were measured in the same membrane while the 1.35 V data were measured in another preparation.

Pulse length Δt	Pore size and number, voltage of the pulse					
	1.35 V		1.45 V		1.6 V	
	w_0/kT	$N/10^5$	w_0/kT	$N/10^5$	w_0/kT	$N/10^5$
0.1 ms					7.7	1
0.2 ms					7.5	2
0.5 ms			6.5	0.6	6.3	4
2 ms	7.5	0.2	5.3	2		
5 ms	7.3	0.4				
10 ms	6.9	0.8				

means of Eqn. 12 shows that the mean pore radius is in the order of 0.6–1 nm ($w_0 = 5$–$8\ kT$).

The modification with increasing pulse length of the dependence of ln G on U is shown in Fig. 9 and Fig. 10. It is worth mentioning that a change of w_0 of 1 kT leads to a substantial increase of the pore conductivity. According to Eqn. 11 the conductivity under low voltages ($n\beta U < w_0$) is increased to the 3-fold. Nevertheless, the observed pores can be regarded as small: the conductivity is strongly dependent on voltage (Fig. 9). The formation of large pores, which practically show an ohmic behaviour was observed only after very long pulses.

In Fig. 10 the dependence of ln G on U is shown after a pulse of 100 ms and 1 Volt. Under these conditions the conductivity is nearly independent of voltage. The pore radius is much bigger in comparison with the conditions described above. This is also shown by the decrease of w_0 to about 2 kT.

An increase of the voltage of the pulse increases the rate of pore creation in the membrane (Table I). This effect was discussed in detail above.

Fig. 11 shows how the dependence of ln G on U is modified in the process of pore resealing after the pulse. In the course of a few milliseconds the membrane conductivity is significantly reduced. Nevertheless the number of pores in the membrane, calculated according to the model considered above, remains constant, indicating that the decrease of conductivity results from a reduction of pore size rather than from a decrease of the number of pores. 10 seconds after the test pulse the conductivity measured at low voltages is reduced to less than 10% of the value measured immediately after the test pulse. The mean pore radius reduces to $R \approx 0.5$ nm ($w_0 \approx 8.4\ kT$).

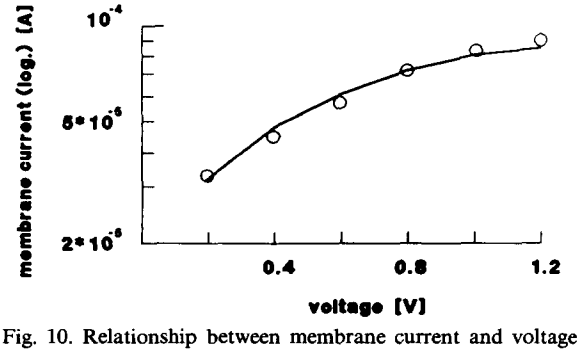

Fig. 10. Relationship between membrane current and voltage immediately after a pulse of 1 V, 100 ms. The conductivity undergoes only little changes. The fit provides an energy barrier of only 1.8 kT.

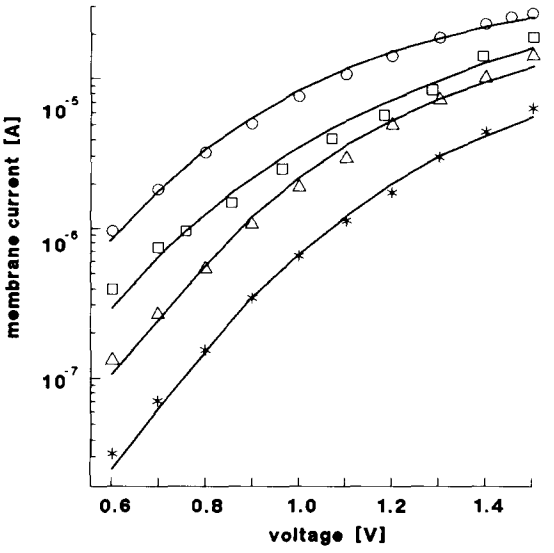

Fig. 11. Relationship between membrane current and voltage at different times after pulses of 1.45 V, 2 ms. ———, fitted according to Eqn. 10.

Symbol	○	□	△	*	Unit
Resealing time [a]	0	2	20	10000	ms
Energy barrier w_0 [b]	5.3	6.6	7.4	8.4	kT
Number of pores [b]	2	2	2	2	$\times 10^5$

[a] Interval between the end of the test pulse and the beginning of the measuring pulse.
[b] Data provided by least-squares fit.

The decrease of the number of pores in the membrane has rather long time constants τ_r (up to more than 10 s). It is much slower than the initial decrease of pore size (1–10 ms). This result is in a good agreement with the estimation of $\tau_r \approx 3$ s made above. The formation of long-living small ($R \approx 0.5$ nm) pores after reversible electric breakdown was reported also by other authors [22,24] who observed resealing times τ_r from seconds to hours.

The long τ_r are due to an energy barrier which prevents the gradual decrease of pore size leading the pore to disappear. The existence of this barrier is obviously connected with the increase of the energy of a hydrophilic pore at small radii (Fig. 4). A reorientation has to take place as in the case of

pore formation. Since τ_r depends exponentially on the height of the energy barrier, it is extremely sensitive to the composition and structure of the membrane. Consequently, variations in τ_r for different membranes may be very large.

Action of lysophosphatidylcholine

The question about the structure of pores determining membrane conductivity in the course of reversible electric breakdown is repeatedly discussed in the literature [1,4–10]. This paper is based on the assumption that the increase in membrane conductivity is caused by hydrophilic rather than hydrophobic pores. Hydrophobic pores play the role of short-living intermediate structures only. The increase of the rate of lipid exchange between the two monolayers observed during breakdown [25], and long life times of pores after breakdown [22,24] support the hypothesis about the hydrophilic structure of the pores. An additional evidence is obtained in the present paper by means of lysophosphatidylcholine treatment of the membranes.

After the addition of less than 0.5 μg/ml lysophosphatidylcholine to the membrane bathing solutions a significant acceleration of the current increase was observed when identical voltage pulses were applied to the membrane. 30 minutes after the addition of 5 μg lysophosphatidylcholine per ml the rate of current increase during pulses of 1.25 V was about 50-times higher than in the untreated membrane.

The acceleration of the current increase is explained by a higher rate of pore creation resulting from a decrease of the energetic barrier for hydrophilic pore formation.

Involvement of lysophosphatidylcholine in hydrophilic pores is energetically favourable because the hydrophobic tail is small in comparison to the hydrophilic head so that the lipid fits to the high curvature of the monolayer in the pore. This effect was predicted theoretically [16,19] and demonstrated experimentally [19] in other systems. When the energy of small hydrophilic pores is decreased, the energetic barrier for the formation of these pores is also decreased.

General aspects

Let us summarize the basic statements of the presented description of reversible electric breakdown in uranyl modified BLM. The increase in conductivity during and after breakdown results from the formation of hydrophilic pores. The defects are formed as a result of inversion of spontaneously arising hydrophobic pores when their sizes grow up to a critical value of about 0.5 nm. To form hydrophilic pores an energy barrier corresponding to the energy of the critical-size hydrophobic pore has to be overcome. The height of this barrier decreases by an amount proportional to the square of membrane voltage. As a result the rate of pore formation is exponentially dependent on U^2. The voltage applied also causes a gradual increase of the mean size of the hydrophilic pores.

Ions crossing the membrane through narrow pores have to overcome an energetic barrier the height of which also depends on membrane voltage. Consequently, the conductivity of the membrane is a non-linear function of voltage. Besides, the current-voltage characteristic significantly depends on the mean size of the pores. The voltage influences the number, the mean size, and the conductivity of the pores, thus.

There are three processes with different time constants determining the changes in membrane conductivity after breakdown. Instantaneously (< 2 μs [20]) with the change of the applied voltage a steep conductivity decrease (or increase) occurs due to the nonlinear, nonohmic character of pore resistance. The number and size of pores remains constant. Then, within approximately 1–10 ms, the mean radius of the pores gradually decreases to $R \approx 0.5$ nm. The resultant small pores are long-living due to an energy barrier preventing their closing. The disappearance of pores takes seconds.

The simplified theory presented is not able to describe all special aspects of the breakdown and resealing behaviour observed in the experiments [28]. Most deviations from 'ideal' membrane properties result from limitations of the model:

The membrane is described as a continuous laterally homogeneous film although the number of lipids forming a pore is very small.

Metastable pore formation is described by first-order kinetics. The possibility of a multistep character of the process has not been taken into account.

We should stress that the presented description of pore formation is not restricted to artificial membranes. There is convincing evidence now that the reversible electric breakdown of cell membranes proceeds mainly through formation of hydrophilic pores in the lipid matrix [22,25,26]. The evidence has been obtained by comparison of main features of breakdown in cell and lipid membranes. Although the consequences of electric breakdown observed in cell and lipid membranes may differ widely, at potential differences of a few 100 mV the electric properties are analogous [22] because of the common mechanism of pore formation.

In cells, however, it need not be the only mechanism; e.g. the Na^+/K^+-ATPase was found under certain conditions to be responsible for up to a third of the voltage-dependent conductivity increase in erythrocyte membranes [27]. Proteins also influence the electric properties indirectly. They stabilize cell membranes against breakdown, but becoming involved into the pore edge proteins slow down resealing. Pore formation may be facilitated at lipid-protein junctions [25].

The breakdown characteristics described (exponential dependence on U^2 etc.) are not antagonistic to the appearance in the membrane system of a critical 'breakdown voltage' which was found in most natural objects. In turn, an exponential dependence of the rate of pore formation on voltage necessarily results in a sharp break in the electric behaviour of the system at a certain current density [29]. This break in the electric behaviour is produced by the rapid increase of voltage drop in the solutions around the membrane.

Other authors interpreted the experimental findings of this critical voltage as sudden changes in the properties of the membrane [1,10,26] and concluded that it should be caused by other mechanisms of pore formation [10]. However, it has been shown theoretically and experimentally that qualitative changes of membrane properties at the 'breakdown voltage' are an artifact [28,29]. The realization of these relations is of considerable importance for the interpretation and practical application of electroporation techniques. The differences between natural membranes and the artificial membranes employed seem to be quantitative rather than qualitative ones; they result from interaction with membrane proteins in cellular membranes as well as from influences of solvent and uranyl ions in the membranes investigated in this study.

The given theory of pore formation and development gains practical relevance to understand the fundamental mechanisms of electric breakdown in electrofusion and electroincorporation techniques.

Appendix

The theoretical model of hydrophobic interaction, proposed by Marcelja [12] is applied to the calculation of σ_o and E_o. It is assumed that the water structure near the hydrophobic surface can be described by a scalar parameter η: at the interface $\eta = \eta_0$, but in the bulk phase $\eta = 0$. The energy of interaction between hydrophobic surface and water can be expressed as [12],

$$E = \int [\eta^2 + \rho^2 (\text{grad } \eta)^2] \, dV \tag{A1}$$

with integration over the volume of water in the pore. η is determined by the minimum of E at fixed boundary conditions.

We introduced cylindric coordinates (z, r, φ) where z is the axis of symmetry of the pore. In small pores ($R \ll h$) one can assume that η differs from zero only inside the pore, where $\eta = \eta(r)$. Thus, from conditions of minimal E_o we get,

$$\eta = \frac{\rho^2}{r} * \frac{d}{dr} r \frac{d}{dr} \eta \tag{A2}$$

Solving Eqn. 2 with the boundary conditions $\eta(R) = \eta_0$ we get η inside the pore,

$$\eta(r) = \eta_0 \frac{I_0(r/\rho)}{I_0(R/\rho)} \tag{A3}$$

where I_n are modified Bessel functions of n-th order: $I_n(r) = i^{-n} J_n(ir)$. From Eqns. A1 and A3 the energy of the hydrophobic pore E_o is

$$E_o = 2\pi h \rho \eta_0^2 R \frac{I_1(R/\rho)}{I_0(R/\rho)} \tag{A4}$$

Determined in an analogous way the energy of interaction of an isolated planar hydrophobic

surface with water is $\rho\eta_0^2 = \sigma_0(\infty)$. Accordingly, Eqn. (A4) can be written in the form

$$E_o(R) = 2\pi hR\sigma_0(R) \tag{A5}$$

where

$$\sigma_0(R) = \sigma_0(\infty)\frac{I_1(R/\rho)}{I_0(R/\rho)} \tag{A6}$$

Expression (A6) provides the change in the effective value of σ_0 that results from hydrophobic interaction of the pore walls.

Acknowledgements

We wish to thank Professor Yu.A. Chizmadzhev, Dr. I.G. Abidor, Dr. S.I. Sukharev and Dr. E. Donath for continuous support and helpful discussions.

References

1 Zimmermann, U. and Vienken, J. (1982) J. Membrane Biol. 67, 165–182.
2 Bates, G., Saunders, J. and Sowers, A.E. (1987) in Cell Fusion (Sowers, A.E., ed.), pp. 367–395, Plenum Press, New York.
3 Vladimirov, Yu.A., Putvinsky, A.V., Puchkova, T.V. and Parnev, O.M. (1983) Stud. Biophys. 94, 115–116.
4 Petrov, A.G., Mitov, M.D. and Derzhnansky, A.I. (1980) in Advances in Liquid Crystal Research and Applications, pp. 695–737, Oxford/Budapest.
5 Pastushenko, V.F. and Petrov, A.G. (1984) in 7th School on Biophysics of Membrane Transport, pp. 70–91, School Proc. Wroclaw.
6 Dimitrov, D.S. (1984) J. Membr. Biol. 78, 53–60.
7 Powell, K.T., Derrick, E.G. and Weaver, J.C. (1986) Bioelectrochem. Bioenerg. 15, 243–255.
8 Sugar, I.P. and Neumann, E. (1984) Biophys. Chem. 19, 211–225.
9 Chernomordik, L.V., Sukharev, S.I., Abidor, I.G., Chizmadzhev, Yu.A. (1983) Biochim. Biophys. Acta 736, 203–213.
10 Benz, R., Beckers, F. and Zimmermann, U. (1979) J. Membr. Biol. 48, 181–204.
11 Israelachvili, J.N. and Pashley, R.M. (1984) J. Coll. Interface Sci. 98, 500–514.
12 Marcelja, S. (1977) Croat. Chem. Acta 49, 347–357.
13 Taupin, C., Dvolaitzky, M. and Sautery, C. (1975) Biochemistry 14, 4771–4775.
14 Abidor, I.G., Arakelyan, V.B., Chernomordik, L.V., Chizmadzhev, Yu.A., Pastushenko, V.F. and Tarasevich, M.R. (1979) Bioelectrochem. Bioenerg. 6, 37–52.
15 Pastushenko, V.F., Chernomordik, L.V. and Chizmadzhev, Yu.A. (1985) Biologiceskie Membrany (in Russian) 2, 813–819.
16 Markin, V.S. and Kozlov, M.M. (1985) Biologiceskie Membrany (in Russian) 2, 205–223.
17 Rand, R.P. (1981) Annu. Rev. Biophys. Bioeng. 10, 277–314.
18 Harbich, W. and Helfrich, W. (1979) Z. Naturforsch. 34a, 1063–1065.
19 Chernomordik, L.V., Kozlov, M.M., Melikyan, G.B., Abidor, I.G., Markin, V.S. and Chizmadyhev, Yu.A. (1985) Biochim. Biophys. Acta 812, 643–655.
20 Chernomordik, L.V., Sukharev, S.I., Abidor, I.G. and Chizmadzhev, Yu.A. (1982) Bioelectrochem. Bioenerg. 9, 149–155.
21 Pastushenko, V.F. and Chizmadzhev, Yu.A. (1982) Gen. Physiol. Biophys. 1, 43–52.
22 Chernomordik, L.V., Sukharev, S.I., Popov, S.V., Abidor, I.G., Pastushenko, V.F., Sokirko, A.V. and Chizmadzhev, Yu.A. (1987) Biochim. Biophys. Acta 902, 360–373.
23 Parsegian, V.A. (1975) Ann. N.Y. Acad. Sci. 264, 161–174.
24 Kinosita, K. and Tsong, T.Y. (1977) Biochim. Biophys. Acta 471, 227–242.
25 Dressler, V., Schwister, K., Haest, C.W.M. and Deuticke, B. (1983) Biochim. Biophys. Acta 732, 304–307.
26 Benz, R. and Zimmermann, U. (1980) Bioelectrochem. Bioenerg. 7, 723–739.
27 Teissié, J. and Tsong, T.Y. (1980) J. Membr. Biol. 55, 133–140.
28 Glaser, R.W. (1986) Thesis, Humboldt-University of Berlin, G.D.R.
29 Glaser, R.W. (1986) Stud. Biophys. 116, 77–86.